Composites: Part B 56 (2014) 477–483

Contents lists available at ScienceDirect

Composites: Part B

journal homepage: www.elsevier.com/locate/compositesb

Acoustic emission analysis for characterisation of damage mechanisms in fibre reinforced thermosetting polyurethane and epoxy

M. Kempf*, O. Skrabala, V. Altstädt

University of Bayreuth, Universitätsstraße 30, D-95447 Bayreuth, Germany

ARTICLE INFO

Article history:
Received 22 May 2013
Received in revised form 25 July 2013
Accepted 26 August 2013
Available online 6 September 2013

Keywords:
D. Acoustic emission
D. Mechanical testing
B. Fatigue
A. Polymer–matrix composites (PMCs)
Thermosetting polyurethane

ABSTRACT

Acoustic emission analysis is used to investigate microscopic damage mechanisms and damage progress in unidirectional glass and carbon fibre reinforced composites. Under static loading the influence of fibre orientation on damage initiation and propagation is determined. A novel polyurethane matrix system significantly enhances material performance in terms of crack initiation load levels, crack growth, damage tolerance and off-axis tensile strength. Hysteresis measurements during stepwise increasing dynamic load tests highlight the effect of fibre–matrix-adhesion and resin fracture toughness in unidirectional 0° fibre reinforced composites. Acoustic detection of beginning fibre breakage correlates with a significant increase of loss work per cycle.

1. Introduction

In the last decades the use of fibre reinforced plastics (FRP) in engineering applications has increased dramatically. The biggest advantage of FRPs is their superior specific strength and stiffness. Starting in space and aeronautic industries, FRPs are nowadays used for lightweight structures in automotive, as well as marine and wind turbine industry. For the design of FRP structures knowledge about damage behaviour is essential to prevent failure during service life. Generally, mechanical testing methods are used to investigate the performance and failure characteristics of FRP. Unfortunately, most static testing methods only provide information about final failure without giving an insight in the initiation process and propagation of damage. To overcome this limitation, acoustic emission (AE) combined with frequency analysis and pattern recognition techniques is a promising approach. By the use of AE analysis crack initiation and propagation can be detected online during mechanical testing. Based on frequency composition of acoustic signals different damage mechanisms as matrix cracking, interphase failure and fibre breakage are distinguishable, even under dynamic loading.

First AE analysis in the field of fibre reinforced composites was done in the 1970s [1–4]. Activities were expanded in the 1980s but analysis was focused on the detection of damage onset, fracture activity and intensity. Correlations between acoustic signals and fracture mechanisms as matrix cracking, fibre breakage and interphase failure were not possible due to insufficient knowledge about physical backgrounds and inapplicable analysis techniques. The identification of different microscopic damage mechanisms succeeded in the mid 1990s by means of determination of the maximum in frequency spectra of AE signals. Matrix cracks show lowest, interphase failure a higher and fibre breakage highest peak frequencys [5,6]. But also sensor response, specimen geometry and sensor location are shown to have some influence on frequency composition of recorded AE signals [7,8]. Therefore, other features in addition to peak frequency are required in order to obtain reliable frequency based discriminations of failure mechanisms in composites.

Indeed, further investigations showed that the entire frequency composition of an AE signal is characteristic for the underlying failure mechanism. Characteristic frequency spectra can be attributed to density and stiffness of the materials involved [10,11]. Furthermore, the application of pattern recognition techniques [12] helps to improve the validity of AE analysis. It is useful to combine several frequency-based features for identification and classification of various failure mechanisms. Fig. 1 shows typical frequency spectra of the three basic microscopic damage mechanisms in fibre reinforced composites: fibre breakage, matrix cracking and interphase failure. Classification procedure itself is described more in detail in Section 2.5.

State of the art mechanical testing of composites has only limited explanatory power regarding damage evolution until final failure. In particular, it is not possible to determine the load levels at

* Corresponding author. Tel.: +49 906719160.
E-mail addresses: manuel.kempf@uni-bayreuth.de (M. Kempf), altstaedt@uni-bayreuth.de (V. Altstädt).
URL: http://polymer-engineering.de (V. Altstädt).

1359-8368/$ - see front matter © 2013 Elsevier Ltd. All rights reserved.
http://dx.doi.org/10.1016/j.compositesb.2013.08.080

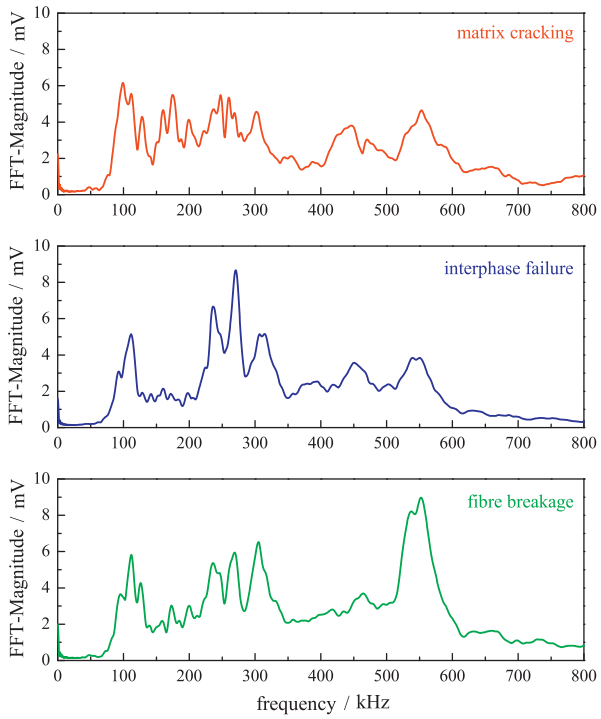

Fig. 1. Frequency spectra of matrix cracking, interphase failure and fibre breakage in glass fibre reinforced polyurehtane. After classification of the acoustic signals recorded during testing, average FFTs are calculated from the respective waveforms by AWARE++ software [9]. Average frequency spectra shown here correspond to acoustic signals emitted from one tensile specimen during testing.

which first microcracking occurs within the material. Furthermore, it is not clear which components are getting damaged and how crack propagation develops. Therefore, this study focuses on microscopic failure mechanisms of glass and carbon fibre reinforced composites under quasi-static as well as under dynamic loading. The investigation of different fibre and matrix combinations by means of acoustic emission analysis during mechanical testing allows to reveal basic structure-properties-relationships concerning fibre–matrix interaction in composite materials. Combining AE analysis with static and dynamic testing of fibre reinforced composites helps to establish a fundamental understanding of their failure behaviour by detailed analysis of microscopic damage mechanisms.

2. Experimental

2.1. Materials

Matrix systems used were a two part standard epoxy/amine infusion resin EPR L 1100 + EPH 294 (EP) from MOMENTIVE and a novel thermosetting polyurethane formulation (PU) provided by Henkel AG & Co. KGaA. Glass fibre (GF) reinforced laminates were made of unidirectional SAERTEX noncrimp fabric (E-Glass) with an areal weight of 701 g/m^2. Carbon fibre (CF) laminates were reinforced by a 244 g/m^2 SAERTEX unidirectional HTS noncrimp fabric.

2.2. Processing and sample preparation

Unidirectional glass and carbon fibre reinforced laminates were manufactured by VARTM-process. Laminate thickness of 2 mm corresponds in both cases – GFRP and CFRP laminates – to fibre volume contents of about 54%. Pre-cut dry textiles were placed in an aluminium RTM-tool, which is afterwards clamped together and heated in a hydraulic hot press. Before injection, the two-part resin systems were stirred in a laboratory mixer and degassed after being homogenously mixed. A curing cycle of four hours at 90 °C was chosen for complete curing of both resin systems. Quality assurance was done by visual inspection for the GFRP laminates and with ultrasonic C-scans for the CFRP laminates. Tensile testing samples were prepared with end tabs according to ISO 527-5 [13] and cut out from the laminates with a circular diamond saw. Deviant to ISO standard a sample width of 20 mm was chosen for proper attachment of the piezo AE sensors. Specimens were prepared from unidirectional reinforced laminates with distinct fibre orientations between 0° and 90° to the direction of load applied to the specimen during testing.

2.3. Static testing

Static tensile tests were conducted in a Zwick 1475 universal testing machine with hydraulic clamping fixtures. Crosshead speed of 0.5 mm/min was chosen for a better differentiation of the single AE signals. Strain measurement was done with an extensometer (Fig. 2). Each series consists of five tested valid specimens. For collecting acoustic signals during testing two AE sensors were clamped onto the specimens with silicon grease as coupling medium. Testing conditions were 23°C and 50% relative humidity.

2.4. Dynamic testing

Dynamic testing was carried out in an Instron Schenk IPLH50K servo-hydraulic testing machine under laboratory conditions (23 °C and 50% r.h.). Tension–tension fatigue tests were performed as stepwise increasing load tests at 1 Hz testing frequency with stress controlled sinusoidal loading and a stress ratio of $R = 0.1$. Strain was measured by means of piston displacement of the servo hydraulic testing machine. First load level was at 100 MPa maximum stress per cycle. For each of the following load levels maximum stress was increased by 100 MPa (Fig. 10). 100 MPa recovery levels inserted between the stepwise increasing load levels allow comparing specimens actual conditions in terms of dynamic modulus and loss work with their initial, undamaged state at 100 MPa maximum stress. Cycle number per load level was 5000 and 1250 for recovery levels.

2.5. Acoustic emission setup

Acoustic emission signals were detected with a PCI-2 AE-System and AEWin software from Physical Acoustics. Two wideband

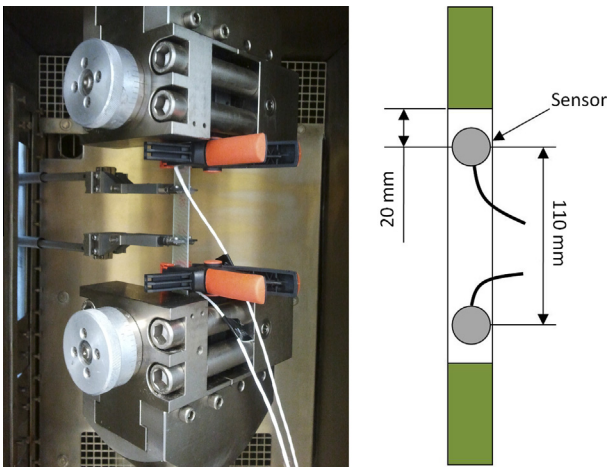

Fig. 2. Static testing setup. Strain is measured by an extensometer (left). Two AE sensors are clamped to the sample at defined positions (right).

WD-sensors are used in case of static loading (Fig. 2) for filtering noise signals from outside of the sample volume. Only signals which could be localised between both AE sensors were recorded. Sensitivity threshold for static testing was 36 dB, sampling rate 10 MHz and frequency range was restricted to 100–1000 kHz, matching sensor bandwith. For dynamic testing no AE signal localisation was carried out and the sensitivity threshold was increased to 60 dB due to continuous noise signals from hydraulic actuation of the dynamic testing machine. Noesis Software was used for post processing and classification of the recorded AE signals.

Pattern recognition techniques were applied by k-means algorithm for AE signal classification in terms of different damage mechanisms. The classification procedure was investigated with several different features, feature-sets and numbers of classes. Features taken into consideration were chosen relating to literature [8,14], whereby it should be noted that frequency spectra and especially peaks observed in within them (Fig. 1) do not result only from recorded AE signals but also from frequency response and peaks in sensor sensitivity. WD-sensors used in this study show at around 270 kHz, 410 kHz and 530 kHz sensitivity peaks, which are consequently reflected in the depicted frequency spectra. In order to consider the entire frequency spectrum recorded, appropriate classification features have to be extracted from acoustic signals. In Table 1, features are listed which finally were selected and found to generate valid classification results.

Partial Power 1–3 correspond to frequency ranges characteristic for matrix cracking, interphase failure and fibre breakage. $f_{centroid}$ reveals information about frequency composition, but does not distinguish between specific damage events. It is therefore combined with characteristic f_{peak} to the damage classification feature f_{WPF}. Classification procedure is identical for static and dynamic testing. In order to enhance the performance of the classification algorithm, features were normalised to their variance [15] and projected to their principal component axes.

For determination of a significant number of different classes we followed the procedure descibed in [16], which evaluates clustering results in terms of cluster compactness and distance between clusters. Similar to results reported in [8], an optimum number of three classes was found. Refering to considerations [10,17] that – in simplified terms – matrix cracking features lower frequencys whereas fibre breakage emits higher frequencys due to higher modulus, these three classes were assigned to the three basic microscopic damage mechanisms in composites: fibre breakage, matrix cracking and interphase failure.

With unsupervised k-means algorithm, three possible classes and the chosen features, good classification results were obtained independent of fibre–matrix-combination or loading direction. For visualisation, two clustering results from 20° off-axis tensile testing of glass fibre reinforced polyurethane and epoxy are shown in Fig. 3. The two principal component axes of these scatterplots correspond to the features 'weighted peak frequency' and 'partial power 2'.

Table 1
Frequency based signal classification features.

Feature	Definition
Peak frequency	Maximum of frequency spectrum (f_{peak})
Weighted peak frequency	$f_{WPF} = \sqrt{f_{peak} \cdot f_{centroid}}$
	$f_{centroid} = \int f \cdot A(f)df / \int A(f)df$
	$A(f)$: Amplitude at frequency f
Partial power 1	0–250 kHz (fraction of frequency spectrum)
Partial power 2	250–450 kHz
Partial power 3	450–800 kHz

3. Results and discussion

3.1. Static testing – different directions of load

Already acoustic emission analysis in its simplest way provides interesting informations about the formation of first cracks within the materials tested. Fig. 4 shows the tensile strenghts of unidirectional glass fibre reinforced EP and PU resin under different loading directions (solid lines). Furthermore, stresses are depicted corresponding to the beginning of damage detected with AE analysis (dashed lines). For all loading directions interphase failure is identified as first damage mechanism occuring. Composite specimens were tested at several angles αbetween fibre orientation and direction of load ($0° \leqslant \alpha \leqslant 90°$).

Under fibre-parallel (0°) tensile loading damage initiation is detected on the same stress level for PU-GF and EP-GF. Ultimate tensile strengths are equal as well. Influence of matrix and interphase properties on strength and onset of first damages become visible at the 10°-off-axis tensile specimens. For angles $\geqslant$20°effects of matrix and interphase are evident. From $\alpha \geqslant 30°$, there is the remarkable observation that damage initiation in the PU based composite is detected at stresses above the tensile strength of EP-GF. This fact is of particular relevance for composite applications. Generally, multiaxial laminates are loaded in a way, that always stresses occur which do not act parallel to fibre orientation. For the PU composite, crack formation range is shifted to higher loadings and, hence, offers considerable lightweight construction potential. The decreasing off-axis tensile strengths with increasing angle between load direction and fibre orientation (Fig. 4) can be described by fits proportional to $1/sin\alpha$.

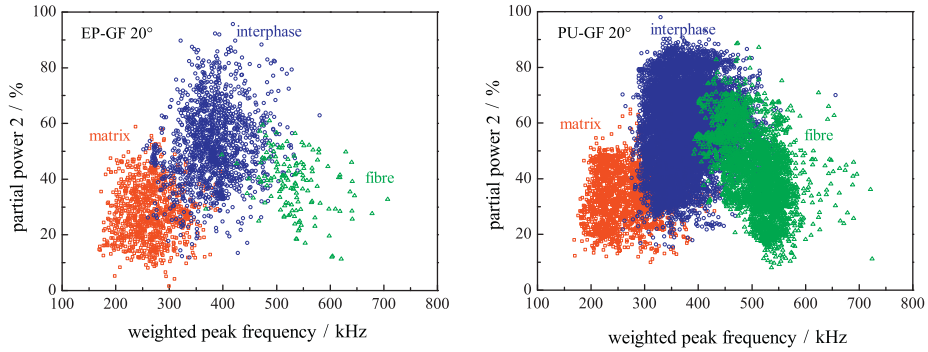

Fig. 3. Clustering results from 20° off-axis tensile testing of glass fibre reinforced epoxy (left) and polyurethane (right). In these scatterplots each datapoint represents an acoustic signal, characterised by the two features 'weighted peak frequency' and 'partial power 2'. Corresponding stress strain diagrams and overall numbers of acustic signals are shown in Fig. 6.

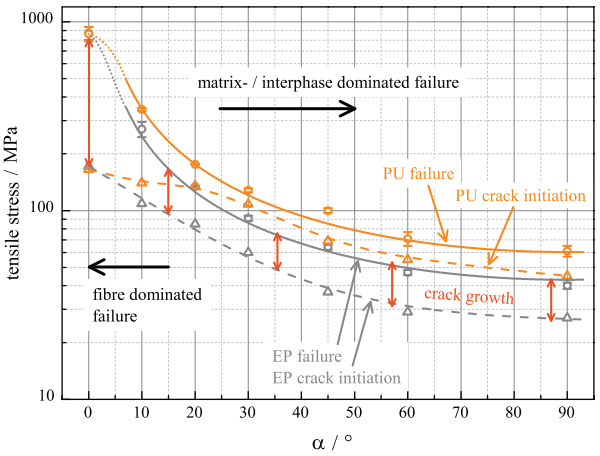

Fig. 4. Tensile strengths and beginning of damage in unidirectional glass fibre reinforced Epoxi (EP) and Polyurethane (PU). Data points were generated for several angles between load direction and fibre orientation.

3.2. Microscopic damage mechanisms – GFRP

When loaded in parallel direction, composites mechanical properties are mainly dominated by the fibres. Therefore, the stress–strain diagrams of glass fibre reinforced EP and PU matrices show almost equal course (Fig. 5). In both cases first damage mechanism detected by AE analysis is interphase failure, followed by fibre breakage. In the epoxy based composite first matrix cracking is detected at around 0.5% strain; in its PU counterpart matrix cracking starts between 0.7% and 0.8% tensile strain. Due to lower fracture toughness of the EP system ($K_{Ic} = 0.75$ MPa $\sqrt{m}$) cracks starting from the interphase grow faster in resin rich regions. In case of the PU system, with its high fracture toughness of around 1.3 MPa $\sqrt{m}$, matrix cracking starts later and less signals are detected until final failure (Fig. 5). Slightly higher failure strain of the PU-Matrix (4.6%) compared to EP (4.2%) promotes this behaviour. Matrix cracks can also induce fibre breakage [18], which is not immediately critical in terms of total failure of the UD ply [19]. This sub-critical fibre breakage until around 700–800 MPa tensile stress is more pronounced in the brittle epoxy composite. Beginning of final failure is observed in both systems at around 800 MPa (or 2% strain) when the rate of detected interphase and fibre failure signals significantly increases.

Off-axis tensile tests were performed to emphasise characteristics and impact of the matrix system used on the composites' overall properties. Fig. 4 showed that the transition from fibre- to matrix/interphase-dominated failure occurs at angles around $\alpha \approx 20°$. In Fig. 6 representative stress–strain diagrams are depicted, obtained from tensile testing at an angle of 20° between load direction and UD fibre orientation, as well as corresponding AE signals. Here, differences between both composites EP and PU resin reinforced with the same glass fibres are clearly visible. The 20° off-axis ultimate tensile strength of the epoxy based composite is 134 ± 1 MPa. First interphase damages within the material are detected already at around 84 MPa tensile stress. Remarkably, first significant acoustic signals of PU-GF are detected at around 135 MPa. At this load level the EP-GF composite already fails (Fig. 6, left).

The low amount of fibre breakage until final failure in EP-GF indicates minor load transfer from the matrix into the fibres. Furthermore, failure strain of the EP-GF composite is far below the glass fibre's failure strain. The small overall number of acoustic signals detected before final failure is another hint for weak interphase. This is confirmed by SEM pictures, which show very smooth and even interphase fracture surface of EP-GF, and correlates well to the comparatively low macroscopic strain to failure. PU-GF fracture surfaces are structured, show barely uncovered fibres but pronounced plastic matrix deformation (Fig. 7). Random fibre matrix debonding in EP-GF leads to unstable propagation of few cracks and localised sudden specimen failure. In contrast, PU-GF emitted an around one order of magnitude higher overall number of interphase failure signals than EP-GF (Fig. 6). This multiple interphase debonding and microcracking is also visually observed (Fig. 8) and and indicates local stress relaxation and stable crack growth. High strain to failure results from this ductile matrix deformation behaviour. Moreover, a considerable load transfer is still maintained into the fibres, what leads to pronounced fibre failure signals even though the 20° off-axis loading state.

3.3. Microscopic damage mechanisms – CFRP

Fig. 9 shows stress–strain diagrams and corresponding acoustic signals obtained from 45° off-axis tensile tested unidirectional carbon fibre reinforced EP and PU. Off-axis tensile performances of the carbon fibre reinforced composites are quite similar to the ones reinforced with glass fibres. Once again, it immediately becomes apparent that under off-axis tensile loading the high strain to failure of PU-CF has to be attributed to plastic deformation of the PU matrix and multiple cracking in the interphase. In addition to higher strain to failure and strength of the PU composites damage initiation thresholds are of particular interest.

Interphase failure, which is again the first damage mechanism detected, begins much earlier in EP-CF. It starts at around 0.6% strain and 60 MPa tesile stress, immediately followed by fibre and matrix breakage. In comparison, the damage initiation range of PU-CF is found at around 85 MPa and 1.4% strain where EP-CF already fails. At this point at the latest, strong adhesion of the PU-matrix to the carbon fibres is evident as well. The overall

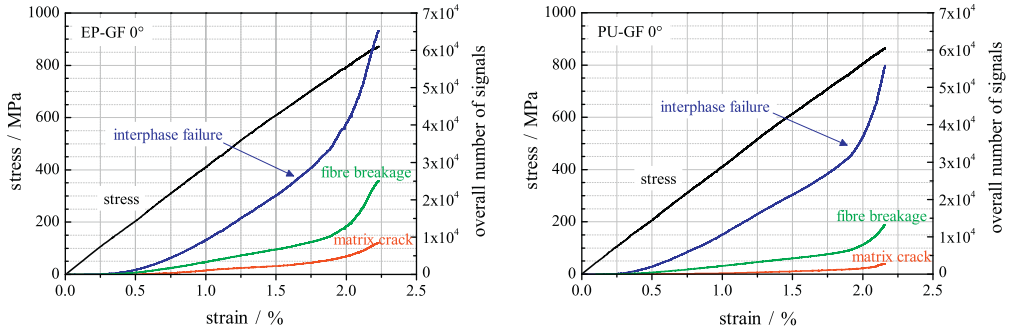

Fig. 5. Quasi-static 0° tensile testing. Stress–strain diagrams and corresponding AE signals for glass fibre reinforced EP (left) and PU (right) look rather similar under fibre-parallel loading.

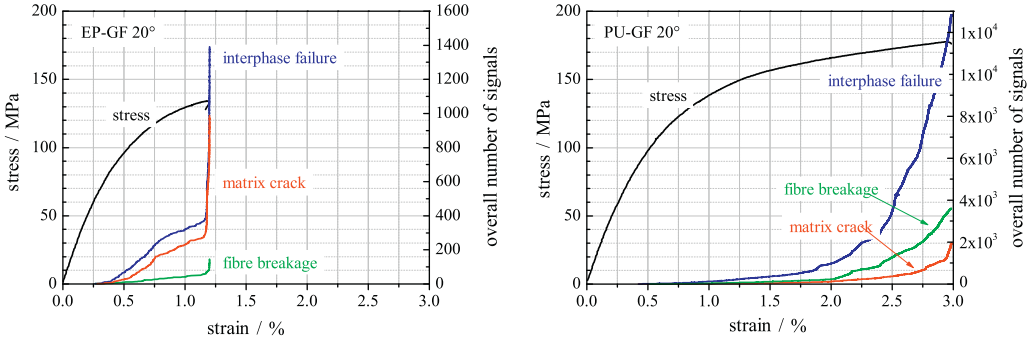

Fig. 6. 20° Off-axis tensile testing stress–strain diagrams of EP-GF (left) and PU-GF (right). Ductile deformation behaviour of the PU resin (right) significantly enhances the composites damage resistance. Much more acoustic signals are detected in PU-GF until final failure.

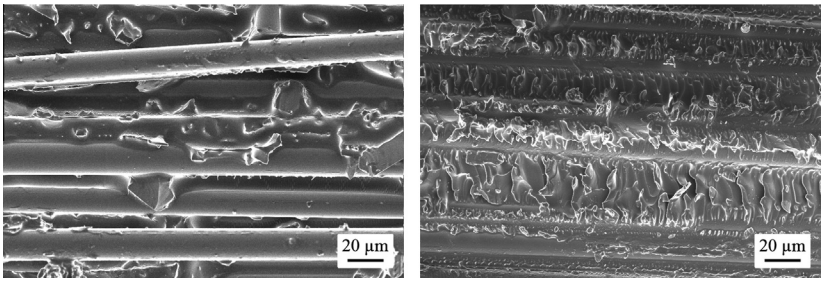

Fig. 7. SEM fracture surface micrographs from 20° off-axis tensile testing samples of EP-GF (left) and PU-GF (right). EP-GF shows a rather smooth fracture surface due to poor fibre–matrix-adhesion. PU-GF instead exhibits strong matrix deformation and good fibre–matrix-adhesion.

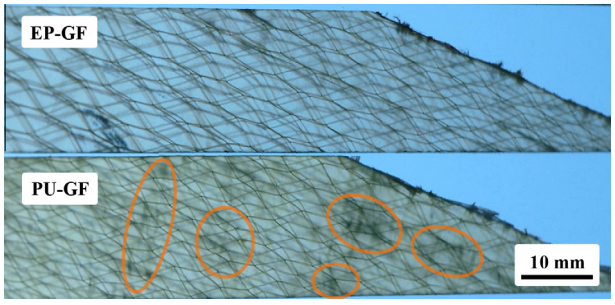

Fig. 8. Visualisation of the fracture behaviour from 20° off-axis tensile testing samples. PU-GF displays opaque spots indicating multiple microcracking before final failure. The 'net structure' seen in specimen's images originates from PES stitching yarn and corresponds to the stitching pattern of the unidirectional glass fibre noncrimp fabric.

number of acoustic signals until final breakdown is relatively low in EP-CF. Whereas PU-CF shows much higher damage tolerance and still a good load transfer into the carbon fibres, since more fibre breakage than matrix cracking is observed (Fig. 9).

3.4. Dynamic testing

As discussed on the basis of Fig. 4, off-axis tensile performance is significantly dependent on the interphase and matrix properties, while the behaviour of EP-GF and PU-GF in 0° quasi-static testing is rather similar. Therefore, dynamic 0° tensile-tensile testing was chosen to investigate the influence of matrix/interphase properties on composite performance under cyclic loading. Hysteresis measurements [20,21] were conducted to determine loss work, which corresponds to the energy dissipated in the material during one load cycle. Increasing loss work indicates proceeding material damage, but reveals not necessarily information about involved damage mechanisms.

Basically, occurring damage mechanisms can be classified under dynamic loading conditions as well, but results are more qualitativ in nature. Continuous background noise of the servo-hydraulic testing equipment prevents, on the one hand,

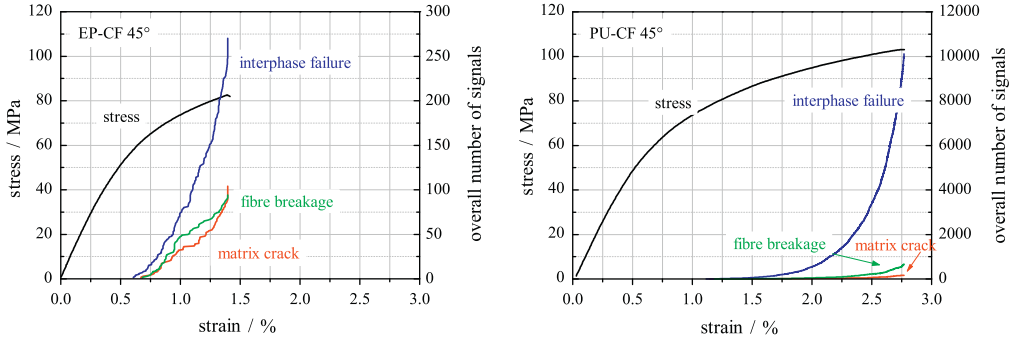

Fig. 9. 45° Off-axis tensile testing with carbon fibre reinforcement. Early unstable interphase failure initiates subsequent fibre breakage and matrix cracking in EP-CF (left). The damage resistance of PU-CF (right) leads to high numbers of recorded AE signals before failure.

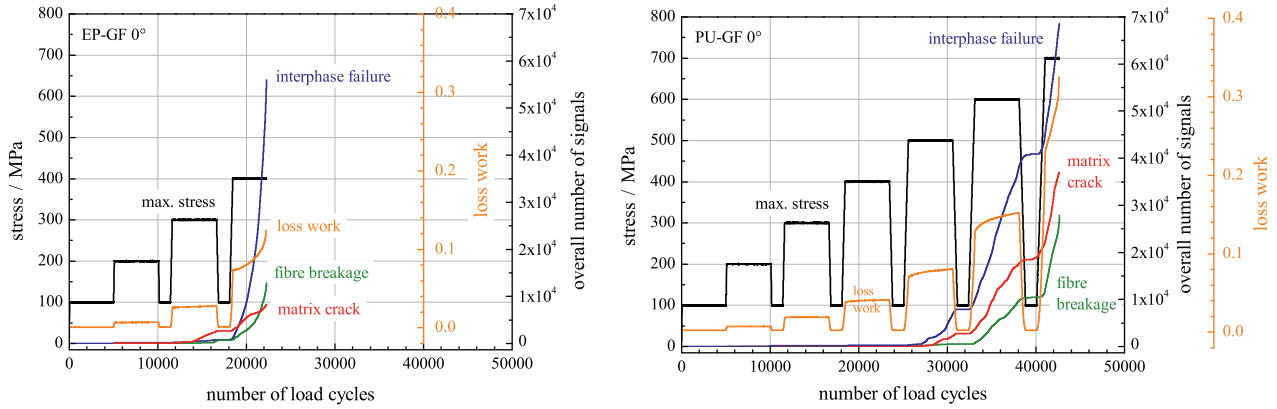

Fig. 10. Stepwise increasing dynamic load tests (0° tension–tension). The EP-GF composite (left) already failed, when damage onset is detected in PU-GF (right).

localisation of acoustic signals; on the other hand, it necessitates a considerable threshold increase for discrete signal identification. Thus, weak signals are not detected, leaving some damage events unconsidered. Nevertheless, with these limitations statements are still possible regarding intensified crack formation and damage evolution, for instance. AE analysis results are in good correlation with the evolution of dynamic modulus and loss work.

As mentioned above, static 0° tensile testing revealed no influence of matrix and interphase on mechanical properties. However, under dynamic loading the use of EP matrix results in significant damage progress at comparatively low load levels. In EP-GF distinct damage onset is observed during the 300 MPa load level (Fig. 10). In this case all three components of the composite are getting damaged. Most signals are matrix cracks, recorded mainly in the second half of the 300 MPa load level. Like during static testing, first interphase failures may induce matrix crack propagation. The material fails during the 400 MPa load level, whose maximum stress is around 46% of the static tensile strength. Analysis of EP-GF's acoustic signals shows steep increase of interphase failure at the beginning of 400 MPa load level. Since, in principal, the reinforcing fibres carry the load, interphase failure cracks along the fibres do not necessarily reduce composite strength. But, at a certain extent, these interphase debondings prevent load transfer to other fibres when local fibre breakage occurs. In case of EP-GF interphase failure is accompanied immediately by a strong increase in fibre breakage. Maximum strain on the 400 MPa load level increases from 1.28% to 1.41%, immediately prior breakdown. This global weakening of the structure due to failure of its reinforcing elements, the fibres, is observed by a dramatic increase in loss work. As can be seen from Fig. 10, loss work is in good correlation to the increasing number of fibre breakage signals.

By comparison, glass fibre reinforced composites based on the novel PU matrix system feature significantly enhanced dynamic damage resistance. First noteworthy acoustic damage signals are recorded during the 500 MPa load level. The EP-GF composite did not even reach this stage. As under quasi-static loading, multiple interphase failure is detected in PU-GF under dynamic loading conditions as well. In contrast to EP-GF the interphase signal number increases more linearly. This again indicates stable crack growth. In addition to clearly visible interphase and matrix signals also a small amount of fibre breakage is observed on the 500 MPa load level, what induces a slight increase in loss work. More heavy fibre failure starts from the beginning of the 600 MPa stage. The material becomes more and more damaged but does not fail within 5000 load cycles, thanks to good fibre matrix adhesion and high toughness. Local damage, in particular fibre failure, is effectively bridged by the PU resin and stresses are transferred again into intact fibre parts. Maximum strain increases from 1.84% to 1.88% during the 600 MPa load level. As a consequence of material damage slight stiffness degradation shows up in the following recovery stage in terms of lower dynamic modulus. Damage accumulation continues at the 700 MPa load level and final failure is announced by a high amount of fibre breakage signals with corresponding increase in loss work.

4. Conclusion

Acoustic emission analysis was performed during static and dynamic tensile testing of glass and carbon fibre reinforced composites. Acoustic signals emitted from the materials can be attributed to fibre breakage, matrix cracking and interphase failure. The different interactions and damage behaviour of glass and carbon fibre in combination with epoxy and polyurethane matrices were investigated. It is shown that material damage always starts in the interphase. Good fibre–matrix-adhesion and matrix toughness lead to damage resistant material behaviour, namely multiple stable and slow microcracking. In case of unstable crack growth initiated by interphase debonding, materials suffer from premature failure under off-axis or dynamic loading. In typical high performance composite applications, materials always have to bear off-axis or dynamic loading. Therefore interphase and matrix properties are crucial for the composites' overall performance. Interphase quality plays a minor role only under 0°quasi-static loading. For other loading conditions interphase and matrix properties are at least as much as important as those of the fibres. The combination of mechanical and dynamic testing with online acoustic emission provides a powerful tool for understanding and optimisation of these basic structure–property-relationships and microscopic damage growth mechanisms in composite materials.

Acknowledgments

The authors thank the Federal Ministry for the Environment, Nature Conservation and Nuclear Safety of the Federal Republic of Germany (BMU) for financial support as well as the project partners (Henkel AG & Co. KGaA, SAERTEX GmbH & Co. KG, Nordex Energy GmbH, ITA Aachen) for providing raw materials and technical support. Research activities were funded in the frame of the Project 0325036D.

References

[1] Fitz-Randolph J, Phillips DC, Beaumont PWR, Tetelman AS. The fracture energy and acoustic emission of a boron–epoxy composite. J Mater Sci 1972;7(3):289–94. http://dx.doi.org/10.1007/BF00555629. <http://link.springer.com/article/10.1007/BF00555629>.

[2] Rotem A, Baruch J. Determining the load–time history of fibre composite materials by acoustic emission. J Mater Sci 1974;9(11):1789–96. http://dx.doi.org/10.1007/BF00541747. <http://link.springer.com/article/10.1007/BF00541747>.
[3] Carlyle JM. Imminent fracture detection in graphite/epoxy using acoustic emission. Exp Mech 1978;18(5):191–5. http://dx.doi.org/10.1007/BF02324141. <http://link.springer.com/article/10.1007/BF02324141>.
[4] Baram J, Rosen M. Fatigue life prediction by distribution analysis of acoustic emission signals. Mater Sci Eng 1979;41(1):25–30. http://dx.doi.org/10.1016/0025-5416(79)90040-5. <http://www.sciencedirect.com/science/article/pii/0025541679900405>.
[5] Gutkin R, Green C, Vangrattanachai S, Pinho S, Robinson P, Curtis P. On acoustic emission for failure investigation in CFRP: pattern recognition and peak frequency analyses. Mech Syst Signal Process 2011;25(4):1393–407. http://dx.doi.org/10.1016/j.ymssp.2010.11.014. <http://www.sciencedirect.com/science/article/pii/S0888327010004176>.
[6] Ramirez-Jimenez C, Papadakis N, Reynolds N, Gan T, Purnell P, Pharaoh M. Identification of failure modes in glass/polypropylene composites by means of the primary frequency content of the acoustic emission event. Compos Sci Technol 2004;64(12):1819–27. http://dx.doi.org/10.1016/j.compscitech.2004.01.008. <http://www.sciencedirect.com/science/article/pii/S0266353804000193>.
[7] Eaton MJ, Holford KM, Featherston CA, Pullin R. Damage in carbon fibre composites: the discrimination of acoustic emission signals using frequency. J Acoust Emission 2007;25:140–8.
[8] Sause MGR, Horn S. Influence of specimen geometry on acoustic emission signals in fiber reinforced composites: FEM-Simulationsand experiments. In: 29th European conference on acoustic emission testing, Vienna; 2010.
[9] Sause MGR. AWARE++ software manual rev. 1.4; 2012. <http://www.physik.uni-augsburg.de/exp2/downloads.de.html/>.
[10] Giordano M, Condelli L, Nicolais L. Acoustic emission wave propagation in a viscoelastic plate. Compos Sci Technol 1999;59(11):1735–43. http://dx.doi.org/10.1016/S0266-3538(99)00035-4. <http://www.sciencedirect.com/science/article/pii/S0266353899000354>.
[11] Sause MGR, Horn S. Simulation of acoustic emission in planar carbon fiber reinforced plastic specimens. J Nondestruct Eval 2010;29(2):123–42. http://dx.doi.org/10.1007/s10921-010-0071-7. <http://link.springer.com/article/10.1007/s10921-010-0071-7>.
[12] Sause M, Gribov A, Unwin A, Horn S. Pattern recognition approach to identify natural clusters of acoustic emission signals. Pattern Recogn Lett 2012;33(1):17–23. http://dx.doi.org/10.1016/j.patrec.2011.09.018. <http://www.sciencedirect.com/science/article/pii/S0167865511002911>.
[13] ISO 527-5:1997, Plastics – determination of tensile properties – Part 5: Test conditions for unidirectional fibre-reinforced plastic composites. Multiple. Distributed through American National Standards Institute (ANSI); 2007.
[14] Sause M, Müller T, Horoschenkoff A, Horn S. Quantification of failure mechanisms in mode-I loading of fiber reinforced plastics utilizing acoustic emission analysis. Compos Sci Technol 2012;72(2):167–74. http://dx.doi.org/10.1016/j.compscitech.2011.10.013. <http://www.sciencedirect.com/science/article/pii/S0266353811003794>.
[15] ENVIROCOUSTICS SA. Noesis advanced acoustic emission data analysis. In: Pattern recognition & neural networks software manual, Rev. 7; 2010.
[16] Anastassopoulos AA, Philippidis TP. Clustering methodology for the evaluation of acoustic emission from composites. J Acoust Emission 1995;13(1–2):11–22. <http://www.refdoc.fr/Detailnotice?idarticle>.
[17] Bohse J. Acoustic emission characteristics of micro-failure processes in polymer blends and composites. Compos Sci Technol 2000;60(8):1213–26. http://dx.doi.org/10.1016/S0266-3538(00)00060-9. <http://www.sciencedirect.com/science/article/pii/S0266353800000609>.
[18] Ehrenstein GW. Faserverbund-Kunststoffe: Werkstoffe – Verarbeitung – Eigenschaften. 2nd ed. KG: Carl Hanser Verlag GmbH & CO; 2006. ISBN:3446227164.
[19] A Puck. Festigkeitsanalyse von Faser-Matrix-Laminaten: Modelle für die Praxis. Hanser Fachbuch; 1996. ISBN:3446181946..
[20] Lazan BJ. Damping of materials and members in structural mechanics. 1st ed. Pergamon Press; 1968. ISBN:0080029345.
[21] Ehrenstein GW. Hysteresis-messverfahren: das flexible Verfahren zur dynamischen Werkstoff- und Bauteilprüfung nach R. Renz. Universität Erlangen-Nürnberg Lehrst. f. Kunststofftechn; 1993. ISBN:3980274047.